

# Migration, Isolation, and Speciation of Hydrothermal Vent Limpets (Gastropoda; Lepetodrilidae) Across the Blanco Transform Fault

SHANNON B. JOHNSON<sup>1</sup>, CURTIS R. YOUNG<sup>1</sup>, WILLIAM J. JONES<sup>1</sup>, ANDERS WARÉN<sup>2</sup>,  
AND ROBERT C. VRIJENHOEK<sup>1,\*</sup>

<sup>1</sup> *Monterey Bay Aquarium Research Institute, 7700 Sandholdt Road, Moss Landing, California; and*

<sup>2</sup> *Swedish Museum of Natural History, Box 50007, SE-10405 Stockholm, Sweden*

**Abstract.** The Sovanco Fracture Zone and Blanco Transform Fault separate the Explorer, Juan de Fuca, and Gorda ridge systems of the northeastern Pacific Ocean. To test whether such offsets in the ridge axis create barriers to along-axis dispersal of the endemic hydrothermal vent animals, we examined the genetic structure of limpet populations previously identified as *Lepetodrilus fucensis* McLean, 1988 (Gastropoda, Lepetodrilidae). Mitochondrial DNA sequences and patterns of allozyme variation revealed no evidence that the 150-km-long Sovanco Fracture Zone impeded gene flow between the Explorer and Juan de Fuca populations. In contrast, the 450-km-long Blanco Transform Fault separates the limpets into highly divergent northern and southern lineages that we recognize as distinct species. We describe southern populations from the Gorda Ridge (Seacliff) and Escanaba Trough as *Lepetodrilus gordensis* new species and refer northern populations from the Explorer and Juan de Fuca ridge systems to *L. fucensis* sensu stricto. The species are similar morphologically, but *L. gordensis* lacks a sensory neck papilla and has a more tightly coiled teleconch. To assess the degree of isolation between these closely related species, we used the Isolation with Migration method to estimate the time of population splitting, effective sizes of the ancestral and derived populations, and rates of migration across the Blanco Transform Fault.

## Introduction

Historically, the deep-sea benthos has been generally considered temporally stable and spatially homogeneous (Gage and Tyler, 1991), factors that should limit opportunities for the geographical isolation and speciation of marine animals (Palumbi, 1992). Hydrothermal vents are notable exceptions, however, because they are distributed as discrete habitat islands along the global mid-ocean ridge system, in back-arc spreading centers, and on seamounts. Tens of kilometers often separate active vent fields along a ridge segment, and hundreds of kilometers can separate adjacent segments. Dispersal among hydrothermal fields occurs primarily through larval or juvenile stages of the invertebrate animals that are sessile or sedentary as adults (Lutz *et al.*, 1984). Thus, vent organisms might be subject to the same kinds of diversifying forces and opportunities for geographical isolation that have made island faunas classical subjects for studies of biodiversity and speciation (Carlquist, 1974; Whittaker, 1998).

Topographical discontinuities of the mid-ocean ridge system (*e.g.*, transform faults, microplates, bathymetric inflation, seamounts) and cross-axis currents can create barriers to along-axis dispersal that promote genetic differentiation and speciation of some vent-endemic animals (France *et al.*, 1992; O'Mullan *et al.*, 2001; Guinot *et al.*, 2002; Guinot and Hurtado, 2003; Won *et al.*, 2003; Hurtado *et al.*, 2004). Yet other vent animals can be genetically homogeneous across the same regions (Shank *et al.*, 1998; Hurtado *et al.*, 2004). Understanding interactions between various dispersal modes of vent animals and geographical factors that promote differentiation *versus* homogenization has been the

Received 22 April 2005; accepted 19 December 2005.

\* To whom correspondence should be addressed. E-mail: [vrijen@mbari.org](mailto:vrijen@mbari.org)

*Abbreviations:* COI, cytochrome *c* oxidase subunit I; HPD, highest posterior density; IM, Isolation with Migration program; TF, transform fault; TMRCA, time of most recent common ancestor.

goal of our studies during the past 15 years (reviewed by Vrijenhoek, 1997).

The present study focuses on vent-endemic limpets (Gastropoda: Lepetodrilidae) from the northeastern Pacific ridge systems (see Fig. 1A). *Lepetodrilus fucensis* was originally described from the Explorer Ridge, west of Vancouver Island, Canada (McLean, 1988), and reported to be abundant at vents on the Juan de Fuca and Gorda ridge systems (Sarrazin and Juniper, 1999; Tsurumi and Tunnicliffe, 2001). However, the present genetic and morphological analysis revealed that Gorda Ridge populations are distinct from *L. fucensis* populations on the Explorer and Juan de Fuca ridges. We name a new species, *Lepetodrilus gordensis* (see appendix), that is sister-species to *L. fucensis* sensu stricto on the basis of an ongoing molecular phylogeny of lepetodrilid limpets (SBJ, unpubl. data). The Blanco Transform Fault (TF), a long fracture zone that formed between 5 and 17 million years ago, separates the two species. To assess whether the Blanco TF might have contributed to vicariance between *L. gordensis* and *L. fucensis*, we used a coalescent-based method to estimate the time of population splitting. Gene flow is assessed within each species, and the potential for introgression between them is considered.

## Materials and Methods

### Specimens

Limpets were collected with manned and unmanned submersibles during numerous oceanographic expeditions (spanning 1988 through 2003) that visited six hydrothermal vent localities (Fig. 1A, Table 1). Once aboard the surface vessel, whole limpets from all but one locality were frozen immediately at  $-80^{\circ}\text{C}$ . Specimens from the Escanaba Trough (NES) were preserved in 95% ethanol. Frozen samples were transported on dry ice to the land-based laboratory and stored at  $-80^{\circ}\text{C}$ . Additional samples used for morphological analyses are listed in the appendix.

### DNA methods

Genomic DNA was isolated using the Qiagen DNeasy DNA extraction kit, following the manufacturer's protocol (Qiagen Inc., Valencia, CA). Approximately 1250 bp of mitochondrial cytochrome *c* oxidase subunit I (*COI*) was amplified with primers based on regions conserved in invertebrates (Nelson and Fisher, 2000) in 157 individual limpets (Table 1).

About 350 bp of the phosphoglucosyltransferase (*Pgm-i*) intron (EC# 5.4.2.2) was amplified with newly designed primers anchored in exon 5 (F) and exon 6 (R) of oyster (aligned with human) regions in 148 individual limpets (Table 1):

PGMF 5'-GCTGCMTTTGATGGAGATGG-3'  
 PGMR 5'-CCACTTGTGGCATACTCC-3'

PCR was conducted in a 25- $\mu\text{l}$  solution that included 30–100 ng of template DNA, 2.5  $\mu\text{l}$  of  $1\times$  PCR buffer (supplied by manufacturer), 2.5  $\mu\text{l}$  of 2.5  $\mu\text{M}$   $\text{MgCl}_2$ , 1  $\mu\text{l}$  of each primer (10  $\mu\text{M}$  final conc.), 2.5 units *Taq* polymerase (Promega Biosciences Inc., Madison, WI), 2.5  $\mu\text{l}$  of 2 mM stock solution of dNTPs, and sterile water to final volume. Amplifications for *COI*, which occurred with a Cetus 9600 DNA thermal cycler (Perkin-Elmer Corp., CT), used an initial denaturation of  $95^{\circ}\text{C}/5$  min, followed by 35 cycles of  $94^{\circ}\text{C}/1$  min,  $55^{\circ}\text{C}/1$  min, and  $72^{\circ}\text{C}/2$  min, and a final extension at  $72^{\circ}\text{C}/7$  min. Amplifications of *Pgm-i*, which occurred with a DNA Engine (PTC-200) Peltier thermal cycler (MJ Research, Inc., Waltham, MA), used an initial denaturation of  $95^{\circ}\text{C}/5$  min followed by 35 cycles at  $94^{\circ}\text{C}/1$  min,  $54^{\circ}\text{C}/1$  min, and  $72^{\circ}\text{C}/2$  min, and a final extension at  $72^{\circ}\text{C}/7$  min. PCR products were purified by gel excision and cleaned with Montage filter units (Millipore Corp., Billerica, MA). PCR products were sequenced bidirectionally with the same primers used in PCR on an ABI 3100 capillary sequencer using BigDye terminator chemistry (Applied Biosystems Inc., Foster, CA). DNA sequences were proofread using Sequencher ver. 4.1 (Gene Codes Corp. Inc., Ann Arbor, MI) and aligned using Clustal X (Thompson *et al.*, 1994) and by eye.

Sequences from the nuclear gene, *Pgm-i*, included individuals that were heterozygous at two or more nucleotide positions. We used two methods to determine the allelic composition of heterozygotes. First, we used the Bayesian statistical method PHASE ver. 2.1 (Stephens *et al.*, 2001; Stephens and Donnelly, 2003) to reconstruct allelic haplotypes from the original sequence traces. To verify these assignments, we used the Topo TA cloning kit (Invitrogen, Carlsbad, CA) to clone PCR products from 31 heterozygous individuals. We sequenced a single colony from each individual to identify one haplotype and then subtracted the cloned haplotype from the ABI traces to resolve the alternate allele.

Statistical analyses of DNA diversity were conducted with *Arlequin* (ver. 2.001, Schneider *et al.*, 2000). A parsimony network of mitochondrial sequences was constructed with the program *TCS* (ver. 1.18, Clement *et al.*, 2000). Appropriate substitution models for *COI* and *Pgm-i* were determined with standard procedures in PAUP (Swofford, 1998) using ModelTest (Posada and Crandall, 1998).

### IM analysis

We used the Isolation with Migration program (IM, Hey and Nielsen, 2004) to estimate population sizes, rates of migration between populations, and time since population splitting (Fig. 2). The Markov chain Monte Carlo (MCMC) method used by IM requires adequate burn-in to achieve convergence (Nielsen and Wakeley, 2001). To improve mixing, we used a two-step heating option with four parallel chains. Approximately  $2 \times 10^8$  steps were sampled from the

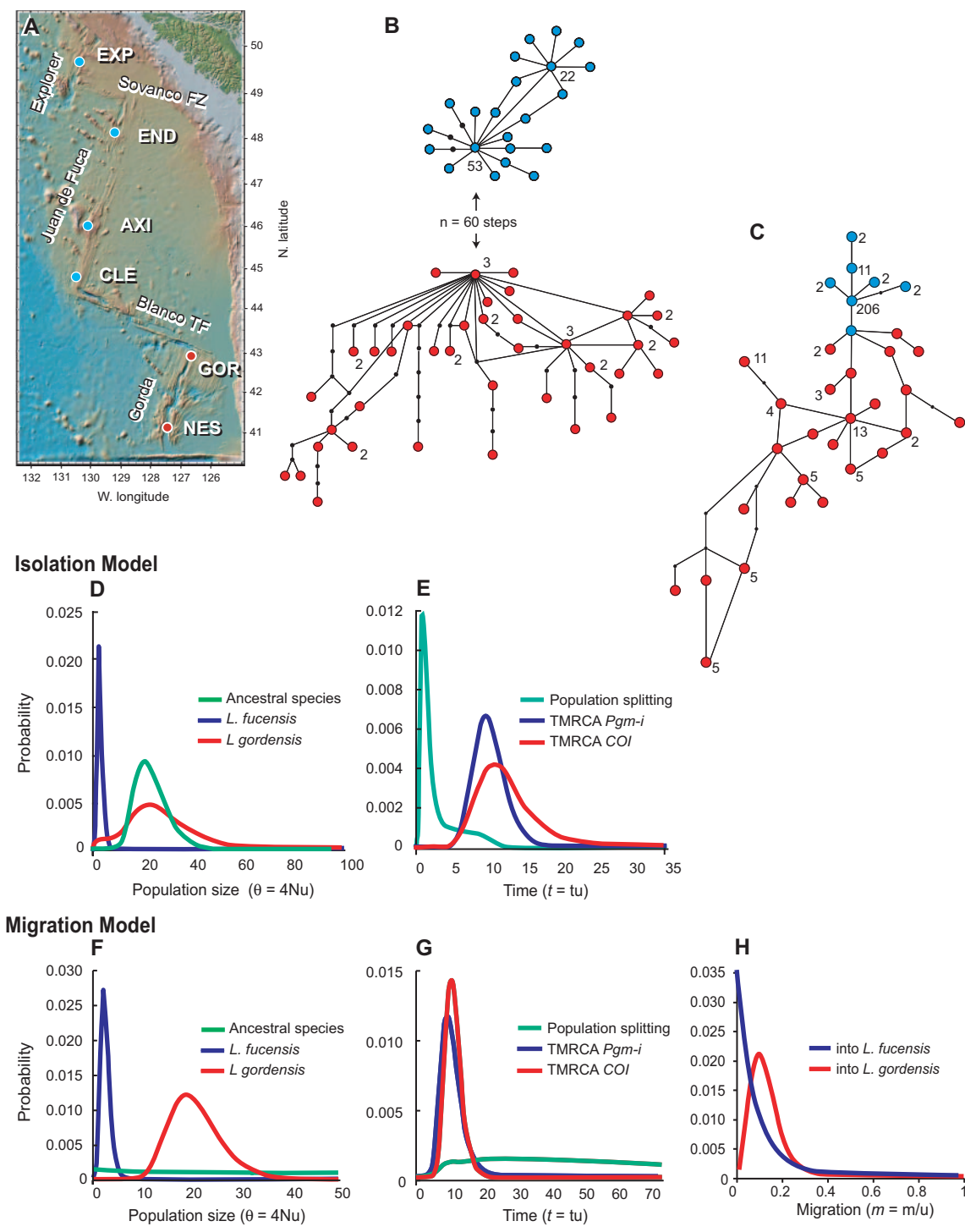


**Figure 1.** *Lepetodrilus* limpets from northeastern Pacific ridge systems. (A) Sample localities along the Explorer (EXP), Juan de Fuca (END, AXI, and CLE), and Gorda (GOR and NES) ridge systems. Maximum parsimony networks for (B) mitochondrial *COI* and (C) nuclear *Pgm-i* haplotype network are separated into blue (northern) and red (southern) haplotypes that segregate across the Blanco Transform Fault. Lines connecting haplotypes based in 95% confidence limit. Black balls represent “missing” haplotypes not seen in sample. Numbers adjacent to each ball represent the sample size for each haplotype. Unnumbered haplotypes were singletons. Posterior probability densities (PPD) for population parameters ( $m$ ,  $\theta$ , and  $t$ ) estimated under the isolation (D and E) and migration (F, G, and H) models, respectively.

Table 1

Northwestern Pacific hydrothermal vent localities, submersible dives, sample dates, and sample sizes of mitochondrial *COI* and nuclear *Pgm-i* sequences and allozymes degrees

Locality	Abbr.	N Lat. <sup>o*</sup>	W Lon. <sup>o*</sup>	Depth (m)	Dive†	Date	# <i>COI</i>	# <i>Pgm-i</i>	# Allozymes
S. Explorer Ridge	EXP	49.761	130.257	1798	R669	07/31/02	4	4	5
		49.759	130.259	1799	R665	07/29/02	4	9	9
		49.760	130.257	1792	R670	07/31/02	4	4	5
Endeavour Segment	END	47.952	129.080	2195	R590	05/11/01	8	8	0
		47.936	129.100	2217	A2068	07/19/88	0	0	30
		47.936	129.858	2202	R591	05/12/01	9	9	0
		47.933	129.100	2265	J059	08/28/03	9	9	0
		47.933	129.083	2200	R710	08/04/03	9	9	0
Axial Volcano	AXI	45.933	129.981	1519	T182	07/28/03	6	7	10
		45.916	130.024	1550	R662	07/20/02	5	6	10
		45.916	129.986	1524	R623	07/20/01	7	7	11
Cleft Segment	CLE	44.990	130.201	2238	T184	07/30/00	17	17	30
		44.933	130.250	2280	A2092	08/20/88	0	0	6
		44.933	130.250	2275	A2075	08/03/88	0	0	10
		44.659	130.364	2202	T458	08/07/02	10	14	42
		44.658	130.363	2211	T180	07/26/00	5	9	30
Gorda Ridge	GOR	42.755	126.708	2716	T186	08/06/00	18	8	30
		42.754	126.709	2715	T188	08/08/00	19	9	30
		42.754	126.709	2723	T454	07/28/02	11	11	0
N. Escanaba Trough	NES‡	41.001	127.495	3222	T452	07/25/02	8	8	0

\* Locations are in decimal degrees.

† Dive numbers are labeled R = *Ropos*; A = *Alvin*; J = *Jason II*, T = *Tiburon*.

‡ Specimens preserved in 95% ethanol; all others frozen.

primary chain after a burn-in of 500,000 steps. We replicated each analysis at least four times, and all replicates yielded similar estimates.

We conducted analyses separately for each gene and then in combined analyses. Because results of the separate analyses were not substantially different, we report the combined analyses. The IM method assumes no recombination and allows two mutation models: infinite sites (IS) and HKY with back mutation (Hasegawa *et al.*, 1985). We used Hudson and Kaplan's (1985) four-gamete test to assess the IS model with no recombination. Either back mutation in the data or recombination may cause a gene segment to fail the four-gamete test. This test simply scans the sequence alignment for pairs of polymorphic sites present in all four possible sample configurations (*e.g.*, (0,0), (0,1), (1,0) and (1,1), where 0 and 1 refer to nucleotide states), and the gene fails the test if one or more pairs of sites are present in all four configurations. *COI* failed the test, and because it is a mitochondrial gene, we assumed that it fit HKY with back mutation. *Pgm-i* also failed, but recombination is likely for a nuclear locus. We used the method of McVean *et al.* (2002) to discriminate back mutation from recombination. Recombination was not supported, so we assumed the HKY model with back mutation for *Pgm-i*, as well. We repeated the analysis, using the largest fragment of *Pgm-i* that passed the four-gamete test (*i.e.*, did not contain pairs of polymorphic sites present in all four possible sample configurations),

and the results were unchanged. We report only the results for the IM analysis using the full *COI* and *Pgm-i* alignments, both assuming the HKY mutation model.

IM scales its estimates of population parameters by the geometric mean of the mutation rates across loci ( $u$ ). To convert IM parameters to more intuitive terms, we estimated substitution rates for *COI* and *Pgm-i* from divergence between *Lepetodrilus tevnianus*, the northwestern Pacific species from the East Pacific Rise (EPR). The EPR and northeastern Pacific ridges (NPR) were once continuous with the Farallon Ridge, which was subducted under the North American Plate about 28.5 million years (MY) ago (Engelbreton and Gordon, 1985; Atwater, 1989). *COI* sequence divergence between *L. tevnianus*, *L. fucensis*, and *L. gordensis* averaged 15.9%, and *Pgm-i* divergence averaged 5.6% (SBJ, unpubl. data), which gives substitution rates of 0.56%/MY for *COI* and 0.20%/MY for *Pgm-i*. The *COI* value is consistent with estimates of divergence rates for this gene between several sister-species pairs of vent-endemic annelids (Chevaldonné *et al.*, 2002), but we have no comparable estimates for *Pgm-i*. Accounting for the different lengths of these gene sequences (*COI* = 1146 bp, *Pgm-i* = 357 bp), and assuming one generation per year, we estimated  $3.2 \times 10^{-6}$  and  $0.35 \times 10^{-6}$  mutations per locus per generation for *COI* and *Pgm-i*, respectively. Their geometrical mean,  $u = 1.06 \times 10^{-6}$ , was used to rescale IM parameters estimated from the combined analysis.

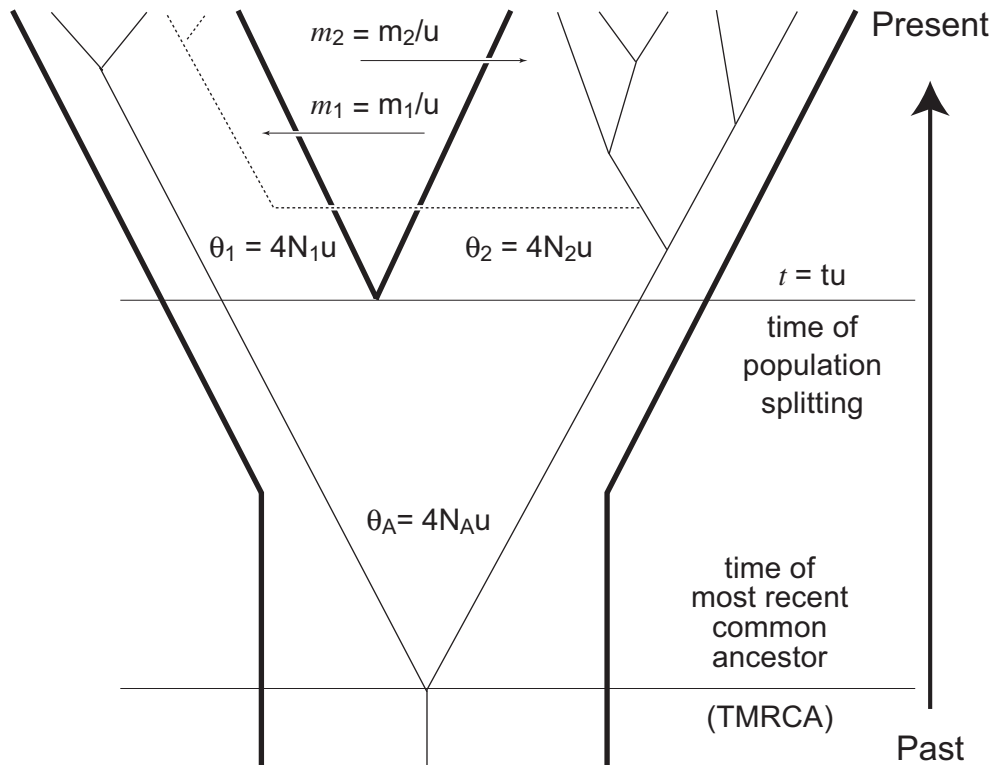


**Figure 2.** Hypothetical gene genealogy superimposed on Isolation with Migration (IM) model. The thin lines trace a genealogy contained within population boundaries defined by the thick lines. The dashed branch depicts immigration into population-1 from population-2 and *vice versa*. Demographic parameters of the IM model are population sizes ( $N_1$ ,  $N_2$ , and  $N_A$ ), gene flow rates per gene copy per generation ( $m_1$  and  $m_2$ ), and time of population splitting,  $t$  generations in the past, all scaled by the neutral mutation rate  $u$  (Wakeley and Hey, 1997; Hey and Nielsen, 2004).

### Allozyme methods

Allozymes encoded by nine loci were examined from five population samples that were frozen in the field (Table 1). Soft tissues from each limpet were homogenized in a roughly equal volume of extraction buffer to tissue (0.01 M Tris, 2.5 mM EDTA, pH 7.0). The homogenate was centrifuged at  $8,000 \times g$  for 2 min to remove tissue debris. We used cellulose acetate gel electrophoresis (CAGE) to screen specimens for multilocus allozymes that had previously been characterized in *Lepetodrilus* (Craddock *et al.*, 1997). Electrophoretic conditions, buffers, and stains followed Herbert and Beaton (1989) unless otherwise noted (Table 2). Statistical analyses of allozyme data were conducted with *Genepop*, (ver. 3.3, Raymond and Rousset, 1995). Exact tests of Hardy-Weinberg frequencies were conducted for loci that exhibited at least two copies of the alternative (less frequent) allele in the total sample.

## Results

### DNA sequence variation

Mitochondrial cytochrome *c* oxidase subunit I (*COI*) DNA sequences (1146 bp) from 153 limpets revealed 64 haplotypes.

*COI* sequences were deposited in GenBank as DQ228006–DQ228070. Phosphoglucumutase intron (*Pgm-i*) sequences (357 bp) from 149 limpets revealed 33 haplotypes. *Pgm-i* sequences were deposited in GenBank as DQ228071–

**Table 2**

*Enzymes assayed and buffers used for allozyme analyses*

Enzyme	Locus	EC No.	Buffers*
6-Phosphogluconate dehydrogenase	<i>Pgdh-I</i>	1.1.1.44	TC 7.0
Aspartate aminotransferase	<i>Aat</i>	2.6.1.2	CA 6.2
Isocitrate dehydrogenase	<i>Idh</i>	1.1.1.42	CA 6.2
Leucine aminopeptidase	<i>Lap</i>	3.4.11.1	TG 8.5
Malic dehydrogenase	<i>Mdh</i>	1.1.1.37	CA 6.2
Mannose-6-phosphate isomerase	<i>Mpi</i>	5.3.1.8	CA 6.2
Peptidase	<i>Pep-la</i>	3.4.11	TG 8.5
Phosphoglucose isomerase	<i>Pgi</i>	5.3.1.9	TC 7.0

\* The chemical compositions of each buffer make up to one liter as follows: TC 7.0: Trizma base (90.8 g), citric monohydrate (52.5 g), pH = 7.0, and dilution factor for working buffer with de-ionized water (20 $\times$ ); TG 8.5: Trizma base (30 g), glycine (144 g), pH = 8.5, and dilution factor (10 $\times$ ); CA 6.2: Citric acid monohydrate (42 g), *N*-(3-aminopropyl)-morpholine (50 ml), pH = 6.2, and dilution factor (20 $\times$ ).

DQ228104. Base compositions for both genes were slightly AT rich (Table 3).

Haplotypic variation was used to create a maximum parsimony network for each gene. The *COI* network identified two clades (Fig. 1B), separated by 60 substitutions. Population samples from north of the Blanco TF (EXP, END, AXI, and CLE) composed one clade (blue in Fig. 1B), and population samples from south of the Blanco TF (GOR and NES) composed the other (red). The *Pgm-i* network also discriminated between the northern and southern populations (Fig. 1C), but the two groups were not reciprocally monophyletic.

We identified an appropriate substitution model for each gene (Table 3). The mean *COI* divergence (HKY+ss model) between northern and southern clades ( $0.0729 \pm 0.0005$  SD) greatly exceeded divergence within either clade (north mean =  $0.0005 \pm 0.0003$  and south mean =  $0.0034 \pm 0.0000$ ). Similarly, mean *Pgm-i* divergence (GTR+I+G model) across the Blanco TF ( $0.0116 \pm 0.0002$ ) was minimally 3-fold greater than divergence within the northern or southern groups (north mean =  $0.0006 \pm 0.0005$ , and south mean =  $0.0069 \pm 0.0000$ ).

Populations south of the Blanco TF exhibited consistently higher diversity for both genes (Table 4). Mean haplotypic diversity ( $\bar{H}$ ) for *COI* across the southern populations was 1.4 times greater than in the northern populations, and mean nucleotide diversity ( $\bar{\pi}$ ) was 21 times greater. Similarly,  $\bar{H}$  for *Pgm-i* was 5.8 times greater in the southern populations, and  $\bar{\pi}$  was 17 times greater.

#### Allozyme variation

Genotypic frequencies within population samples conformed to random mating expectations, and single-locus fixation indices ( $f_i$ ) were not significantly different from zero. No evidence existed for deviations from random mating expectations, as the multilocus observed ( $H_o$ ) and expected ( $H_e$ ) heterozygosities were not significantly different (Table 4).

Northern and southern groups of populations separated by the Blanco TF exhibited fixed differences for *Aat-2* and *Lap-2*, and nearly fixed differences existed for *Idh*, *Mdh-1*

and *Pgi*. Nei's unbiased genetic distance (Nei, 1978) between the northern and southern groups was 0.821, which contrasts with genetic distances within groups that were not significantly greater than zero.

Except for one locality, allozyme diversity was low in the northern populations (Table 4). Allelic richness and heterozygosity were higher at CLE because this population had rare alleles at four loci that were common alleles south of the Blanco TF at GOR (Table 5). Note, however, that the sample from CLE was much larger than samples from the other populations, so we expected to detect more rare alleles. Heterozygosity was greatest in the GOR sample, due to evenness of the *Mpi* alleles.

#### Ridge offsets and population subdivision

To assess whether large ridge offsets correspond with genetic divergence, we estimated pairwise  $F_{ST}$  values between all population samples (Table 6). No significant differentiation in *COI*, *Pgm-i*, or allozymes existed between the two northern populations (EXP and END) separated by the Sovanco Fracture zone. For these genetic markers, the four northern populations (EXP, END, AXI, and CLE) composed a single homogeneous group (pairwise  $F_{ST}$  values for all loci  $< 0.043$ ). In contrast, these nuclear and cytoplasmic markers revealed highly significant subdivision (pairwise  $F_{ST}$  values for all loci 0.550–0.983) between populations on either side of the Blanco TF. The southern populations (GOR and NES) differed significantly from all the northern populations for cytoplasmic and nuclear markers, but unlike northern populations, they were not completely homogeneous and showed some subdivision between localities. *COI* frequencies differed significantly between GOR and NES ( $F_{ST} = 0.051$ ;  $P = 0.009$ ). Despite this slight subdivision between southern localities, species-level differences were found across the Blanco TF where 5 of 9 allozyme loci and *Pgm-i* were fixed or nearly fixed, and *COI* was reciprocally monophyletic.

#### Systematics

The levels of divergence between the northern (EXP, END, AXI, and CLE) and southern (GOR and NES) limpet

Table 3

Maximum likelihood estimates of substitution model parameters\*

	-lnL	Base frequencies				Rate matrix					Rate variation			
		pA	pC	pG	pT	k	R(a)	R(b)	R(c)	R(d)	R(e)	c <sub>1</sub>	c <sub>2</sub>	c <sub>3</sub>
<i>COI</i> (HKY+ss)	2444.1	0.27	0.22	0.17	0.34	12.34						0.19	0.00	2.81
<i>Pgm-i</i> (GTR+I+G)	837.0	0.31	0.18	0.20	0.31	7.80	6.21	3.21	2.09	6.40		l	a	
												0.69	0.88	

\*  $p_i$  = equilibrium frequency of nucleotide base  $i$ ;  $k$  = ts/tv rate ratio;  $c_i$  = relative rate ratios at 1st, 2nd, and 3rd nucleotide positions in codon  $i$ ;  $R(i)$  = GTR rate matrix as in PAUP v. 4.0;  $l$  = proportion of invariant sites; and  $a$  = gamma shape parameter.

Table 4

Estimates of genetic variation for *Lepetodrilus* populations; error estimates (one standard deviation) in parentheses

Gene	Parameter*	<i>L. fucensis</i>				<i>L. gordensis</i>	
		EXP	END	AXI	CLE	GOR	NES
<i>COI</i>	<i>N</i>	15	35	18	31	46	8
	<i>H</i>	7	8	6	7	37	5
	<i>h</i>	0.81 (0.075)	0.577 (0.086)	0.699 (0.090)	0.527 (0.099)	0.988 (0.008)	0.857 (0.108)
	$\pi$	0.00116 (0.00086)	0.00076 (0.00061)	0.00081 (0.00067)	0.00068 (0.00057)	0.00417 (0.00230)	0.03148 (0.01752)
<i>Pgm-i</i>	<i>N</i>	34	70	42	80	56	16
	<i>H</i>	1	3	5	4	21	11
	<i>h</i>	0 0.000	0.111 (0.050)	0.343 (0.092)	0.188 (0.057)	0.927 (0.016)	0.933 (0.048)
	$\pi$	0 0.0000	0.0003 (0.0006)	0.0015 (0.0014)	0.0005 (0.0008)	0.0097 (0.0060)	0.0104 (0.0060)
Allozymes	<i>n</i>	18.8 (0.10)	30 0.00	30.1 (0.30)	116.6 (0.70)	59.6 (0.20)	ND ND
	<i>A</i>	1.1 (0.10)	1.1 (0.10)	1.2 (0.10)	1.6 (0.20)	1.2 (0.10)	ND ND
	<i>P</i>	11.1	11.1	0	11.1	11.1	ND
	<i>H<sub>o</sub></i>	0.012 (0.012)	0.004 (0.004)	0.011 (0.008)	0.026 (0.015)	0.028 (0.026)	ND ND
	<i>H<sub>e</sub></i>	0.011 (0.011)	0.011 (0.011)	0.011 (0.008)	0.025 (0.014)	0.033 (0.031)	ND ND

\* *N* = sample size per locus; *H* = number of haplotypes; *h* = haplotype diversity;  $\pi$  = nucleotide diversity; *n* = mean sample size; *A* = mean number of alleles per locus; *P* = percentage of polymorphic loci; *H<sub>o</sub>* = observed heterozygosity; and *H<sub>e</sub>* = expected heterozygosity. Refer to Table 1 for location abbreviations. ND indicates no data.

populations greatly exceed the levels of divergence found within either subdivision. Concordant divergence across multiple gene loci provides a useful indicator of long-standing subdivision and, thus, provides an operational evolutionary criterion for the recognition of species boundaries (Avice and Wollenberg, 1997). The observed level of *COI* divergence between the northern and southern groups (7.3%) is consistent with species-level divergence seen in a survey of *Lepetodrilus* species worldwide (6%–9%; SBJ, unpubl. data). Similarly, *Pgm-i* sequence divergence between *L. fucensis* and *L. gordensis* (1.12%) is comparable to that found in other sister-species pairs such as *L. elevatus* and *L. galriflensis* (SBJ, unpubl. data). The number of allozyme loci examined was small, but again the genetic distance between *L. fucensis* and *L. gordensis* (Nei's *D* = 0.821) was consistent with species-level divergence (Vrijenhoek *et al.*, 1994; Craddock *et al.*, 1995).

On the basis of divergence in these genetic markers and diagnostic morphological characters (see appendix), we recommend that limpets formerly subsumed under the name *Lepetodrilus fucensis* be recognized as allopatric species separated by the Blanco TF: *Lepetodrilus gordensis* new

species (described in appendix) and *Lepetodrilus fucensis* sensu stricto.

#### Analysis of isolation, gene flow, and divergence times

The Blanco TF separates *Lepetodrilus gordensis* and *L. fucensis* s. s. We used the IM program to address whether the time of splitting between these species might be consistent with the age of the Blanco TF. This coalescence-based method is preferred over phylogenetic methods when closely related taxa might still experience limited gene flow (Hey and Nielsen, 2004). The analysis was restricted to the GOR and CLE populations, because these populations flank the Blanco TF, and because other populations within each species were essentially homogenous.

We first examined the Isolation (I) model,  $m_i = 0$  (Fig. 1D and E). Under the I model, the population size of *L. fucensis* ( $N_f = 0.7 \times 10^6$ ; Table 7) was smaller than that of *L. gordensis* ( $N_g = 5.0 \times 10^6$ ), which was similar to the ancestral population ( $N_A = 5.4 \times 10^6$ ). The time of population splitting ( $t = 1.2$  MY) is young, but its 90% highest posterior density (HPD) interval is broad. In addition, the

Table 5

Allelic frequencies at nine allozyme loci

Locus/allele	<i>Lepetodrilus fucensis</i>			<i>Lepetodrilus gordensis</i>	
	EXP	END	AXI	CLE	GOR
<i>Aat-1</i> (N)	19	30	31	118	60
100	1.000	1.000	1.000	1.000	1.000
<i>Aat-2</i> (N)	19	30	31	118	60
100	1.000	1.000	1.000	1.000	0
90	0	0	0	0	1.000
<i>Idh</i> (N)	19	30	30	116	59
100	1.000	1.000	1.000	0.996	0
70	0	0	0	0.004	1.000
<i>Lap-1</i> (N)	19	30	31	118	60
100	1.000	1.000	1.000	1.000	1.000
<i>Lap-2</i> (N)	19	30	31	118	60
100	1.000	1.000	1.000	1.000	0
60	0	0	0	0	1.000
<i>Mdh-1</i> (N)	18	30	29	111	60
100	0	0	0.017	0.005	1.000
70	1.000	1.000	0.983	0.995	0
<i>Mdh-2</i> (N)	19	30	29	117	60
100	1.000	1.000	1.000	0.996	1.000
40	0	0	0	0.004	0
<i>Mpi</i> (N)	19	30	30	117	59
100	0.947	0.950	0.967	0.940	0.831
80	0.053	0.050	0.033	0.060	0.169
<i>Pgi</i> (N)	18	30	29	116	58
100	0	0	0	0.043	0.991
80	1.000	1.000	1.000	0.957	0.009

Refer to Table 1 for location abbreviations.

time mutation-scaled estimator,  $t = tu$  was negatively correlated with  $\theta_A$  ( $r = -0.33$ ). If  $t$  is young,  $\theta_A$  is likely to be large, whereas if  $t$  is older,  $\theta_A$  is likely to be much smaller. Notwithstanding, the upper 90% HPD for  $t$  is 7.4 MY, which is less than the maximum likelihood estimates of time of most recent common ancestor (TMRCA) for *COI* (11.3 MY) and *Pgm-i* (9.4 MY) (Fig. 1E). Under the isolation model, both gene genealogies split well before population splitting, as hypothetically portrayed in Figure 2.

Next we examined the general IM model with  $m_i > 0$  (Fig. 1F–H; Table 7). Rates of gene flow were highly asymmetric, with immigration into *L. gordensis* ( $2N_g m_g = 0.9025$ ) greatly exceeding immigration into *L. fucensis* ( $2N_f m_f = 0.0018$ ). However, population size for *L. gordensis* ( $N_g = 5.4 \times 10^6$ ) was also much greater than for *L. fucensis* ( $N_f = 0.57 \times 10^6$ ). Due to the flat posterior probability densities (Fig. 1F and G), we could not estimate  $N_A$ , size of the ancestral population, or  $t$ , the time of population splitting under the migration model. We were unable to statistically identify the most appropriate demographic model (isolation vs. migration) with the current data.

Table 6

Pairwise  $F_{ST}$  values between population samples of *Lepetodrilus limpets* from northeastern Pacific Ridge systems: *COI* (above diagonal); *Pgm-i* (below diagonal)

Locality	EXP	END	AXI	CLE	GOR	NES
<i>COI</i> (above diagonal)						
and <i>Pgm-i</i>						
(below)						
EXP		0.042	-0.01	0.027	<b>0.949</b>	<b>0.973</b>
END	0.005		-0.006	-0.009	<b>0.960</b>	<b>0.983</b>
AXI	0.043	0.027		-0.017	<b>0.953</b>	<b>0.978</b>
CLE	0.013	-0.005	0.018		<b>0.959</b>	<b>0.983</b>
GOR	<b>0.553</b>	<b>0.629</b>	<b>0.550</b>	<b>0.636</b>		<b>0.051</b>
NES	<b>0.619</b>	<b>0.717</b>	<b>0.577</b>	<b>0.715</b>	0.026	
Allozymes						
EXP		0.000	0.000	0.000	<b>0.839</b>	ND
END			0.000	0.000	<b>0.838</b>	ND
AXI				0.000	<b>0.831</b>	ND
CLE					<b>0.821</b>	ND

Negative values are interpreted as zero. Boldface values are significantly different at  $\alpha = 0.05$ . ND indicates no data. Refer to Table 1 for location abbreviations.

## Discussion

Northeastern Pacific hydrothermal vent limpets previously attributed to a single species, *Lepetodrilus fucensis*, represent two evolutionarily distinct allopatric lineages that we recognize as sister-species, *L. gordensis* new species and *L. fucensis* sensu stricto (appendix). *L. gordensis* is restricted to the Gorda Ridge, and *L. fucensis* s.s. is restricted to the Juan de Fuca and Explorer ridges. *L. fucensis* and *L.*

Table 7

Maximum likelihood estimates (MLE) of population parameters, followed by lower (L) and upper (U) 90% highest posterior density (HPD) from the Isolation with Migration analysis

Parameter	Migration model			Isolation model		
	MLE	L	U	MLE	L	U
$\theta_f$	2.4	0.6	4.1	2.9	1.3	5.4
$\theta_g$	19.0	9.4	28.0	21	13	36
$\theta_A$	0.1	0.1	134.0	23	1.1	51
$t$	24.0	0.04	67.0	1.3	0.34	7.8
$m_f$	0.0015	0.0015	0.2200	†		
$m_g$	0.0950	0.0015	0.2000	†		
$N_f \times 10^6$	0.57	0.15	0.97	0.7	0.3	1.3
$N_g \times 10^6$	4.50	2.20	6.70	5.0	3.0	8.5
$N_A \times 10^6$	*	*	*	5.4	0.3	12.0
$t \times 10^6$ y	22.7	4.0	68.9	1.2	0.3	7.4
$2N_f m_f$	0.0018			0		
$2N_g m_g$	0.9025			0		

\* Not estimable; posterior probability density is flat.

† Set to zero.

*gordensis* were reciprocally monophyletic for highly divergent mitochondrial haplotypes (Fig. 1B). Nuclear gene differences were also evident in phosphoglucosylase intron sequences, but *Pgm-i* haplotypes were not reciprocally monophyletic and interspecific divergence was not as deep as with *COI*. Allozymes also revealed differences between the two species, with fixed differences at two loci, nearly fixed differences at three loci, a frequency shift at one locus, and no observed differences at two electrophoretically monomorphic loci (Table 5).

An ongoing molecular phylogenetic analysis of *Lepetodrilus* species has revealed that *L. fucensis* and *L. gordensis* are each other's closest relatives (SBJ, unpubl. data). *COI* divergence between the two species is 7.3%, and average divergence from their closest known relative (*Lepetodrilus tevniatus* from the East Pacific Rise) is 15.9%. Levels of interspecific *COI* divergence found between species of deep-sea bivalve molluscs, siboglinid tubeworms, and decapod crustaceans typically exceed 4%, whereas intraspecific divergence is less than 2% (Peek *et al.*, 1997; Shank *et al.*, 1998; Guinot *et al.*, 2002; Hurtado *et al.*, 2002, 2004; Goffredi *et al.*, 2003; Won *et al.*, 2003; Rouse *et al.*, 2004).

Various measures of gene diversity were uniformly higher in *L. gordensis* than in *L. fucensis* (Table 4). Higher diversity in Gorda Ridge populations might result from metapopulation processes such as local extinction and recolonization events. Tectonic spreading rates along the Gorda Ridge are characteristically slow (Sleep and Rosen-dahl, 1979), which could minimize population turnover. Conversely, the Juan de Fuca and Explorer ridges are intermediate spreading centers (Sclater *et al.*, 1971; Atwater, 1990), where vent habitats may be more ephemeral. Detailed studies of the stability of vent habitats in these regions are needed to test this hypothesis.

#### Gene flow in northeastern Pacific *Lepetodrilus*

We used different methods to assess rates of gene flow within and between the two species. Standardized variances ( $F_{ST}$ ) in allelic frequencies are inversely related to gene flow ( $Nm$ ) among populations that have achieved an equilibrium for genetic drift and migration ( $F_{ST} = 1/(4Nm + 1)$ ; Wright, 1965). All intraspecific values of  $F_{ST}$ , except one, were small and not significantly different from zero for *COI*, *Pgm-i*, and allozymes (Table 6). The single exception was a significant  $F_{ST} = 0.051$  for *COI* in the North Escanaba Trough/Gorda Ridge (NES/GOR) pair. Notwithstanding, these  $F_{ST}$  values are consistent with very high rates of interpopulational gene flow ( $Nm \geq 9$  migrants per generation) within both species.

The presence of shared *Pgm-i* and allozyme alleles suggests that a low level of gene flow might exist between the two species, or alternatively that the two species have retained ancestral polymorphisms. The  $F_{ST}$  method is not

appropriate for estimating gene flow between species; therefore we applied the multi-locus Isolation with Migration (IM) method (Hey and Nielsen, 2004). If interspecific gene flow exists, it is highly asymmetric (Table 6). Immigration into *L. fucensis* is essentially zero, and immigration into *L. gordensis* is less than one migrant per generation. A southward bias in gene flow might contribute to higher genetic diversity in *L. gordensis*, but IM analysis accounts for this and still reveals that *L. gordensis* has a larger effective population size. Unfortunately, the present data do not allow us to discriminate statistically between models of complete isolation and limited one-way migration. Nevertheless, interspecific gene flow, if it exists, should not be viewed as the antithesis of speciation (*sensu* Mayr, 1963). Molecular analyses suggest that genetic exchange between recently separated species is more common than previously expected (Carson, 1975; Barton and Hewitt, 1989; Hey and Nielsen, 2004). Thus, hybridization and introgression can also be viewed as potentially creative processes that increase genetic variation and augment the scope for adaptive diversification (Endler, 1977; Arnold, 1997; Dowling and Secor, 1997; Grant and Grant, 1994).

Little is known about larval development of lepetodrilid limpets and how barriers like the Blanco Fracture Zone might affect their dispersal. The absence of a protoconch 2, which is formed during a feeding veliger stage, suggests that these limpets possess lecithotrophic veligers, which in turn suggests they their dispersal capability might be limited (Lutz *et al.*, 1986). Population genetic studies of limpets from the East Pacific Rise and Galapagos Rift (Craddock *et al.*, 1997) also suggested that their dispersal rates were less than those of vent-endemic bivalves and annelids (reviewed by Vrijenhoek, 1997). Veligers of *L. fucensis* have been found in buoyant hydrothermal plumes that might transport them along a ridge axis (Mullineaux *et al.*, 1995). On the other hand, cross-axis currents constrained by transform faults, fracture zones, and other ridge discontinuities might transport buoyant larvae away from the ridge axis (Vrijenhoek, 1997; Thomson *et al.*, 2003; Won *et al.*, 2003; Hurtado *et al.*, 2004). Larval abundance of *L. fucensis* was shown to be high both within vent fields at Endeavour (END), Explorer (EXP), and Axial Volcano (AXI) as well as along ridge axes, suggesting that larval supply within ridge segments is localized and larval retention within vent fields and along ridge segments is a significant mechanism for maintaining vent communities (Metaxis, 2004). The Sovanco Fracture Zone, a 150-km-long transform fault that separates EXP and END, did not impede gene flow between *L. fucensis* s.s. populations. In contrast, the Blanco Transform Fault (TF), which is 450-km long, corresponds with a boundary that separates *L. fucensis* from *L. gordensis*. The vent tubeworm *Ridgeia piscesia* shows a parallel pattern of divergence and asymmetrical gene flow across this boundary (Young, unpubl. data). Multispecies patterns of popula-

tion structure and gene flow are indicators of common dispersal filters along the southern East Pacific Rise (Won *et al.*, 2003; Hurtado *et al.*, 2004). although the filters affect species with divergent life histories to varying degrees.

#### *Dating the split between L. gordensis and L. fucensis*

Formation of the Blanco TF might have played a significant role in partially isolating *L. fucensis* and *L. gordensis*. Plate kinematic models suggest that the Juan de Fuca and Gorda ridge axes began to diverge 5–18 MY ago (Riddi-hough, 1984). The Cascadia depression, a large feature of the Blanco TF, formed approximately 5 MY (Farrar and Dixon, 1980; Embley and Wilson, 1992). If the Blanco TF was involved in isolating the two species, molecular estimates for the time of population splitting should not exceed the age of this structure.

We used the IM method to estimate the time ( $t$ ) of population splitting. If we assume that *L. gordensis* and *L. fucensis* have been completely isolated since first splitting from a common ancestor (the I model), then the estimated time of population splitting is recent,  $t = 1.2$  MY (90% HPD interval: 0.3–7.4). On the other hand, if we assume the two species have exchanged migrants since first splitting (the M model), then  $t$  might be much older (90% HPD interval 4.0–68.9 MY). The probability density distribution for  $t$  is flat (Fig. 1H), so we have no confidence in the estimates made under the M model.

It is common practice to date species splits using an estimate of the time of most recent common ancestor (TMRCA) of monophyletic genes. However, we have long appreciated that the timings of splits in gene trees and the timing of splits in species trees do not necessarily coincide in closely related taxa (Arbogast, 2002, and references therein). Several factors determine how TMRCA of genes and the timing of speciation events coincide: (1) the effective size of the ancestral species; (2) the time since the species became isolated; (3) whether migration has or has not been occurring at some low rate; and (4) whether the genes examined are selectively neutral. The TMRCA we estimated from the two gene genealogies were similar ( $Pgm-i = 9.4$  and  $COI = 11.1$  MY). Under the I model, both genes would have split well before the populations split; under the M model, gene and population splitting may have been coincident or the population split may even have preceded the gene splits.

It is clear from the analysis that (1) gene trees may provide poor estimates of the ages of these species; (2) the precision of our estimates of the species split is low under the M model; and (3) the data do not allow us to identify the appropriate demographic model. Unfortunately, our ability to date the species split is highly dependent on the model that we assume. As previously stated, molecular analyses suggest that genetic exchange between recently separated

species is more common than previously expected, and although we failed to reject the null hypothesis of isolation in this case, we had limited statistical power. Additional nuclear genes are needed to discriminate between the two hypotheses. With additional data, the timing of this split may be recoverable even if migration does occur at a low rate.

The isolation and migration models are only two alternatives from a broad range of evolutionary scenarios. For example, the migration model assumes continuous gene flow since population splitting, but it seems more likely that gene flow would attenuate as the ridge offset grows. In addition, rates of gene flow might be irregular due to sporadic megaplumes that carry larvae long distances. Finally, actual dispersal might be higher than estimated from gene flow if the alleles are not adaptively neutral. For example, cytonuclear interactions and selection might prevent mitochondrial introgression, while permitting introgression of some nuclear genes. Different degrees of gene introgression across species-contact zones are believed to reveal underlying strengths of differential selection (Barton and Hewitt, 1985). Though the present data do not allow us to reconstruct the ongoing and historical processes that separated *L. gordensis* and *L. fucensis* with great precision, the data are consistent with the hypothesis that the Blanco Transform Fault plays a significant role in their separation.

#### Acknowledgments

We thank the crews and pilots of the *R/V Western Flyer* and *ROV Tiburon*, and the *R/V Atlantis* and *DSV Alvin* for their technical support and patience. Verena Tunnicliffe, Amanda Bates, and Noreen Kelly kindly shared limpet specimens collected with *ROV Ropos* and ideas and information from their work on *L. fucensis* and commented on an earlier edition of this paper. Janet Voight (funded by NOAA/NURP) sent specimens for comparative purposes. Funding for this project was provided by the Monterey Bay Aquarium Research Institute (The David and Lucile Packard Foundation) and NSF grants (OCE9910799 and OCE0241613).

#### Literature Cited

- Arbogast B. S., S. V. Edwards, J. Wakeley, P. Beerli, and J. B. Slowinski. 2002. Estimating divergence times from molecular data on phylogenetic and population genetic timescales. *Annu. Rev. Ecol. Syst.* 33: 707–740.
- Arnold, M. L. 1997. *Natural Hybridization and Evolution*. Oxford University Press, Oxford, United Kingdom.
- Atwater, T. 1989. Plate tectonic history of the northeast Pacific and western North America, Pp. 21–72 in *The Eastern Pacific Ocean and Hawaii*, Vol. N., E. L. Winterer, D. M. Hussong, and R. W. Decker, eds. Geological Society of America, Boulder, CO.
- Atwater, T. 1990. Tectonics of the Northeast Pacific. *Trans. R. Soc. Can.* 1: 295–318.

- Avise, J. C., and K. Wollenberg. 1997. Phylogenies and the origin of species. *Proc. Natl. Acad. Sci. USA* **94**: 7748–7755.
- Barton, N. H., and G. M. Hewitt. 1985. Analysis of hybrid zones. *Annu. Rev. Ecol. Syst.* **16**: 113–148.
- Barton, N. H., and G. M. Hewitt. 1989. Adaptation, speciation and hybrid zones. *Nature* **341**: 497–503.
- Carlquist, S. 1974. *Island Biology*. Columbia University Press, New York.
- Carson, H. 1975. The genetics of speciation at the diploid level. *Am. Nat.* **109**: 83–92.
- Chevaldonné, P., D. Jollivet, D. Desbruyères, R. A. Lutz, and R. C. Vrijenhoek. 2002. Sister-species of eastern Pacific hydrothermal-vent worms (Ampharetidae, Alvinellidae, Vestimentifera) provide new mitochondrial clock calibration. *Cah. Biol. Mar.* **43**: 367–370.
- Clement, M., D. Posada, and K. A. Crandall. 2000. TCS: a computer program to estimate gene genealogies. *Mol. Ecol.* **4**: 331–346.
- Collin, R. 1995. Size, sex and position: a test of models predicting size at sex change in the protandrous gastropod *Crepidula fornicata*. *Am. Nat.* **146**: 815–831.
- Craddock, C., W. R. Hoeh, R. G. Gustafson, R. A. Lutz, J. Hashimoto, and R. C. Vrijenhoek. 1995. Evolutionary relationships among deep-sea mytilids (Bivalvia: Mytilidae) from hydrothermal vents and cold-water methane/sulfide seeps. *Mar. Biol.* **121**: 477–485.
- Craddock, C., R. A. Lutz, and R. C. Vrijenhoek. 1997. Patterns of dispersal and larval development of archaeogastropod limpets at hydrothermal vents in the eastern Pacific. *J. Exp. Mar. Biol. Ecol.* **210**: 37–51.
- De Burgh, M. E., and C. L. Singla. 1984. Bacterial colonization and endocytosis on the gill of a new limpet species from a hydrothermal vent. *Mar. Biol.* **84**: 1–6.
- Dowling, T. E., and C. L. Secor. 1997. The role of hybridization and introgression in the diversification of animals. *Annu. Rev. Ecol. Syst.* **28**: 593–619.
- Embley, R. W., and D. S. Wilson. 1992. Morphology of the Blanco Transform Fault Zone- NE Pacific: implications for its tectonic evolution. *Mar. Geophys. Res.* **14**: 25–45.
- Endler, J. 1977. *Geographic Variation, Speciation and Clines*. Princeton University Press, Princeton, NJ.
- Engelbreton, D. C., and R. G. Gordon. 1985. *Relative Motions Between Oceanic and Continental Plates in the Pacific Basin*. Special Papers, No. 206, Geological Society of America, Boulder, CO. 59 pp.
- Farrar, E., and J. M. Dixon. 1980. Miocene ridge impingement and the spawning of secondary ridges off Oregon, Washington, and British Columbia. *Tectonophysics* **69**: 321–348.
- France, S. C., R. R. Hessler, and R. C. Vrijenhoek. 1992. Genetic differentiation between spatially-disjunct populations of the deep-sea, hydrothermal vent-endemic amphipod *Ventiella sulfuris*. *Mar. Biol.* **114**: 551–559.
- Fretter, V. 1988. New archaeogastropod limpets from hydrothermal vents; superfamily Lepetodrilacea. II. Anatomy. *Philos. Trans. R. Soc. Lond. B Biol. Sci.* **318**: 33–82.
- Gage, J. D., and P. A. Tyler. 1991. *Deep Sea Biology: A Natural History of Organisms at the Deep-Sea Floor*. Cambridge University Press, Cambridge.
- Goffredi, S. K., L. A. Hurtado, S. Hallam, and R. C. Vrijenhoek. 2003. Evolutionary relationships of deep-sea vent and cold seep clams (Mollusca: Vesicomysidae) of the “*pacifica/lepta*” species complex. *Mar. Biol.* **142**: 311–320.
- Grant, P. R., and B. R. Grant. 1994. Phenotypic and genetic effects of hybridization in Darwin’s finches. *Evolution* **48**: 297–316.
- Guinot, D., and L. A. Hurtado. 2003. Two new species of hydrothermal vent crabs of the genus *Bythograea* from the southern East Pacific Rise and from the Galapagos Rift (Crustacea Decapoda Brachyura Bythograeidae). *C. R. Biologies* **326**: 423–439.
- Guinot, D., L. A. Hurtado, and R. C. Vrijenhoek. 2002. New genus and species of brachyuran crab from the southern East Pacific Rise (Crustacea Decapoda Brachyura Bythograeidae). *C. R. Biologies* **325**: 1119–1128.
- Hasegawa, M., H. Kishino, and T. Yano. 1985. Dating of the human-ape splitting by a molecular clock of mitochondrial DNA. *J. Mol. Evol.* **22**: 160–174.
- Hebert, P. D. N., and M. Beaton. 1989. *Methodologies for Allozyme Analysis Using Cellulose Acetate Gels*. Helena Laboratories, Beaumont, TX.
- Hey, J., and R. Nielsen. 2004. Multilocus methods for estimating population sizes, migration rates and divergence time, with applications to the divergence of *Drosophila pseudoobscura* and *D. persimilis*. *Genetics* **167**: 747–760.
- Hudson, R. R., and N. L. Kaplan. 1985. Statistical properties of the number of recombination events in the history of a sample of DNA sequences. *Genetics* **111**: 147–164.
- Hurtado, L. A., M. Mateos, R. A. Lutz, and R. C. Vrijenhoek. 2002. Molecular evidence for multiple species of *Oasisia* (Annelida: Siboglinidae) at eastern Pacific hydrothermal vents. *Cah. Biol. Mar.* **34**: 377–380.
- Hurtado, L. A., R. A. Lutz, and R. C. Vrijenhoek. 2004. Distinct patterns of genetic differentiation among annelids of eastern Pacific hydrothermal vents. *Mol. Ecol.* **13**: 2603–2615.
- Kim, S.L. and L.S. Mullineaux. 1998. Distribution and near-bottom transport of larvae and other plankton at hydrothermal vents. *Deep-Sea Res.* **45**: 423–440.
- Lutz, R. A., D. Jablonski, and R. D. Turner. 1984. Larval development and dispersal at deep-sea hydrothermal vents. *Science* **26**: 1451–1454.
- Lutz, R. A., P. Bouchet, D. Jablonski, R. D. Turner, and A. Warén. 1986. Larval ecology of mollusks at deep-sea hydrothermal vents. *Am. Malacol. Bull.* **4**: 49–54.
- Mayr, E. 1963. *Animal Species and Evolution*. Belknap Press, Cambridge, MA.
- McLean, J. H. 1988. New archaeogastropod limpets from hydrothermal vents: superfamily Lepetodrilacea. I. Systematic descriptions. *Philos. Trans. R. Soc. Lond. B Biol. Sci.* **319**: 1–32.
- McLean, J. H. 1993. New species and records of *Lepetodrilus* (Vetigastropoda: Lepetodrilidae) from hydrothermal vents. *Veliger* **36**: 27–35.
- McVean, G., P. Awadalla, and P. Fearnhead. 2002. A coalescent-based method for detecting and estimating recombination from gene sequences. *Genetics* **160**: 1231–1241.
- Metaxas, A. 2004. Spatial and temporal patterns in larval supply at hydrothermal vents in the northeast Pacific Ocean. *Limnol. Oceanogr.* **49**: 1949–1956.
- Mullineaux, L. S., P. H. Weibe, and E. T. Baker. 1995. Larvae of benthic invertebrates in hydrothermal vent plumes over the Juan de Fuca Ridge. *Mar. Biol.* **122**: 585–596.
- Nei, M. 1978. Estimation of average heterozygosity and genetic distance from a small number of individuals. *Genetics* **89**: 583–590.
- Nelson, K., and C. Fisher. 2000. Absence of cospeciation in deep-sea vestimentiferan tube worms and their bacterial endosymbionts. *Symbiosis* **28**: 1–15.
- Nielsen, R., and J. Wakeley. 2001. Distinguishing migration from isolation: a Markov Chain Monte Carlo Approach. *Genetics* **158**: 885–896.
- O’Mullan, G. D., P. A. Y. Maas, R. A. Lutz, and R. C. Vrijenhoek. 2001. A hybrid zone between hydrothermal vent mussels (Bivalvia: Mytilidae) from the Mid-Atlantic Ridge. *Mol. Ecol.* **10**: 2819–2831.
- Palumbi, S. R. 1992. Marine speciation in a small planet. *Trends Ecol. Evol.* **7**: 114–117.
- Peek, A., R. Gustafson, R. Lutz, and R. Vrijenhoek. 1997. Evolutionary relationships of deep-sea hydrothermal vent and cold-water seep

- clams (Bivalvia: Vesicomidae): results from the mitochondrial cytochrome oxidase subunit 1. *Mar. Biol.* **130**: 151–161.
- Posada, D., and K. A. Crandall. 1998.** MODELTEST: testing the model of DNA substitution. *Bioinformatics* **14**: 817–818.
- Pradillon F., B. Shillito, C.M. Young, and F. Gaill. 2001.** Developmental arrest in vent worm embryos. *Nature* **413**: 698–699.
- Raymond, M., and F. Rousset. 1995.** GENEPOP (Ver. 1.2): population genetics software for exact tests and ecumenicism. *J. Hered.* **86**: 248–249.
- Riddihough, R. 1984.** Recent movements of the Juan de Fuca plate system. *J. Geophys. Res.* **89**: 6980–6994.
- Rouse, G. W., S. K. Goffredi, and R. C. Vrijenhoek. 2004.** *Osedax*: bone-eating marine worms with dwarf males. *Science* **305**: 668–671.
- Sarrazin, J., and S. K. Juniper. 1999.** Biological characteristics of a hydrothermal edifice mosaic community. *Mar. Ecol. Prog. Ser.* **185**: 1–19.
- Schneider, S., D. Roessli, and L. Excoffier. 2000.** *Arlequin, A Software Package for Population Genetics Data Analysis*. Genetics and Biometry Laboratory, Department of Anthropology, University of Geneva, Geneva.
- Sclater, J. G., R. N. Anderson, and M. L. Bell. 1971.** Elevation of ridges and evolution of the central eastern Pacific. *J. Geophys. Res.* **76**: 7888–7915.
- Shank, T. M., R. A. Lutz, and R. C. Vrijenhoek. 1998.** Molecular systematics of shrimp from deep-sea hydrothermal vents: enigmatic “small orange” shrimp from the Mid-Atlantic Ridge are juvenile *Rimicaris exoculata*. *Mol. Mar. Biol. Biotech.* **7**: 88–96.
- Sleep, N. H., and B. R. Rosendahl. 1979.** Topography and tectonics of mid-oceanic ridge axes. *J. Geophys. Res.* **84**: 6831–6839.
- Stephens, M., and P. Donnelly. 2003.** A comparison of Bayesian methods for haplotype reconstruction from population genotype data. *Am. J. Hum. Genet.* **73**: 1162–1169.
- Stephens, M., N. J. Smith, and P. Donnelly. 2001.** A new statistical method for haplotype reconstruction from population data. *Am. J. Hum. Genet.* **68**: 978–989.
- Swofford, D. L. 1998.** *PAUP\*. Phylogenetic Analysis Using Parsimony (\* and Other Methods)*. Sinauer, Sunderland, MA.
- Thompson, J. D., D. G. Higgins, and T. J. Gibson. 1994.** CLUSTAL W: improving the sensitivity of progressive multiple sequence alignment through sequence weighting, position specific gap penalties and weight matrix choice. *Nucleic Acids Res.* **22**: 4673–4680.
- Thomson, R. E., S. F. Mihály, A. B. Rabinovich, R. E. McDuff, S. R. Veirs, and F. R. Stahr. 2003.** Constrained circulation at Endeavour Ridge facilitates colonization by vent larvae. *Nature* **24**: 545–549.
- Tsurumi, M., and V. Tunnicliffe. 2001.** Characteristics of a hydrothermal vent assemblage on a volcanically active segment of Juan de Fuca Ridge. *Can. J. Fish. Aquat. Sci.* **58**: 530–542.
- Van Dover, C. L., and B. Fry. 1994.** Microorganisms as food resources at deep-sea hydrothermal vents. *Limnol. Oceanogr.* **39**: 51–57.
- Van Dover, C. L., and R. R. Hessler. 1990.** Spatial variation in faunal composition of hydrothermal vent communities on the East Pacific Rise and Galapagos spreading center. Pp. 253–264 in *Gorda Ridge: A Seafloor Spreading Center in the United States' Exclusive Economic Zone*, G. R. McMurray, ed. Springer-Verlag, New York.
- Vrijenhoek, R. C. 1997.** Gene flow and genetic diversity in naturally fragmented metapopulations of deep-sea hydrothermal vent animals. *J. Hered.* **88**: 285–293.
- Vrijenhoek, R. C., S. J. Schutz, R. G. Gustafson, and R. A. Lutz. 1994.** Cryptic species of deep-sea clams (Mollusca, Bivalvia, Vesicomidae) in hydrothermal vent and cold-seep environments. *Deep-Sea Res. Part II* **41**: 1171–1189.
- Wakeley, J., and J. Hey. 1997.** Estimating ancestral population parameters. *Genetics* **145**: 847–855.
- Warén, A., and P. Bouchet. 2001.** Gastropoda and monoplacophora from hydrothermal vents and seeps: new taxa and records. *Veliger* **44**: 116–231.
- Whittaker, R. 1998.** *Island Biogeography: Ecology, Evolution and Conservation*. Oxford University Press, Oxford.
- Won, Y., C. R. Young, R. A. Lutz, and R. C. Vrijenhoek. 2003.** Dispersal barriers and isolation among deep-sea mussel populations (Mytilidae: *Bathymodiolus*) from eastern Pacific hydrothermal vents. *Mol. Ecol.* **12**: 169–184.
- Wright, S. 1965.** The interpretation of population structure by *F*-statistics with special regard to systems of mating. *Evolution* **19**: 395–420.

## Appendix

### Description of *Lepetodrilus gordensis* n. sp.

Superfamily Lepetodrilioidea McLean, 1988.

Family Lepetodrilidae McLean, 1988.

*Lepetodrilus gordensis* new species

Figures 3–5

Previously referred to as: “lepetodrilid limpets” (Van Dover and Hessler, 1990: 285); “*Lepetodrilus fucensis*” (McLean, 1993: 32–34); “Limpet” (Van Dover and Fry, 1994: 53–55).

### Methods

Morphological observations are based on specimens collected in connection with various projects. Specimens were frozen and thawed in ethanol or fixed in 4% formalin and transferred to 70%–80% ethanol. Specimens were not relaxed prior to preservation, making comparisons of organ shapes difficult; therefore, analyses were limited to presence vs. absence of character-states rather than measurements. Radulae were prepared from 6 specimens from both the Juan de Fuca Ridge (*Tiburón* dives: T184 and T458) and the Gorda Ridge (T186 and T188), by dissolving whole bodies in 25% potassium hydroxide. Some 25 specimens or parts of them were critical-point-dried *via* ethanol - carbon dioxide and examined with scanning electron microscopy. Shells of juvenile specimens were cleaned with dilute commercial bleach for examination of the larval shells.

### Material examined

*Lepetodrilus gordensis*, all from the Gorda Ridge:

Type material. Holotype, Swedish Museum of Natural History (SMNH) type collection register number 6074; many paratypes, number 6075 (ex SMNH 78769), from the type locality, *Tiburón* dive T186, Gorda Ridge, 42° 45'N, 126° 42'W, 2716 m; 5 paratypes each at Muséum national d'histoire naturelle, Paris; Los Angeles County Museum of Natural History (LACM 1974); California Academy of

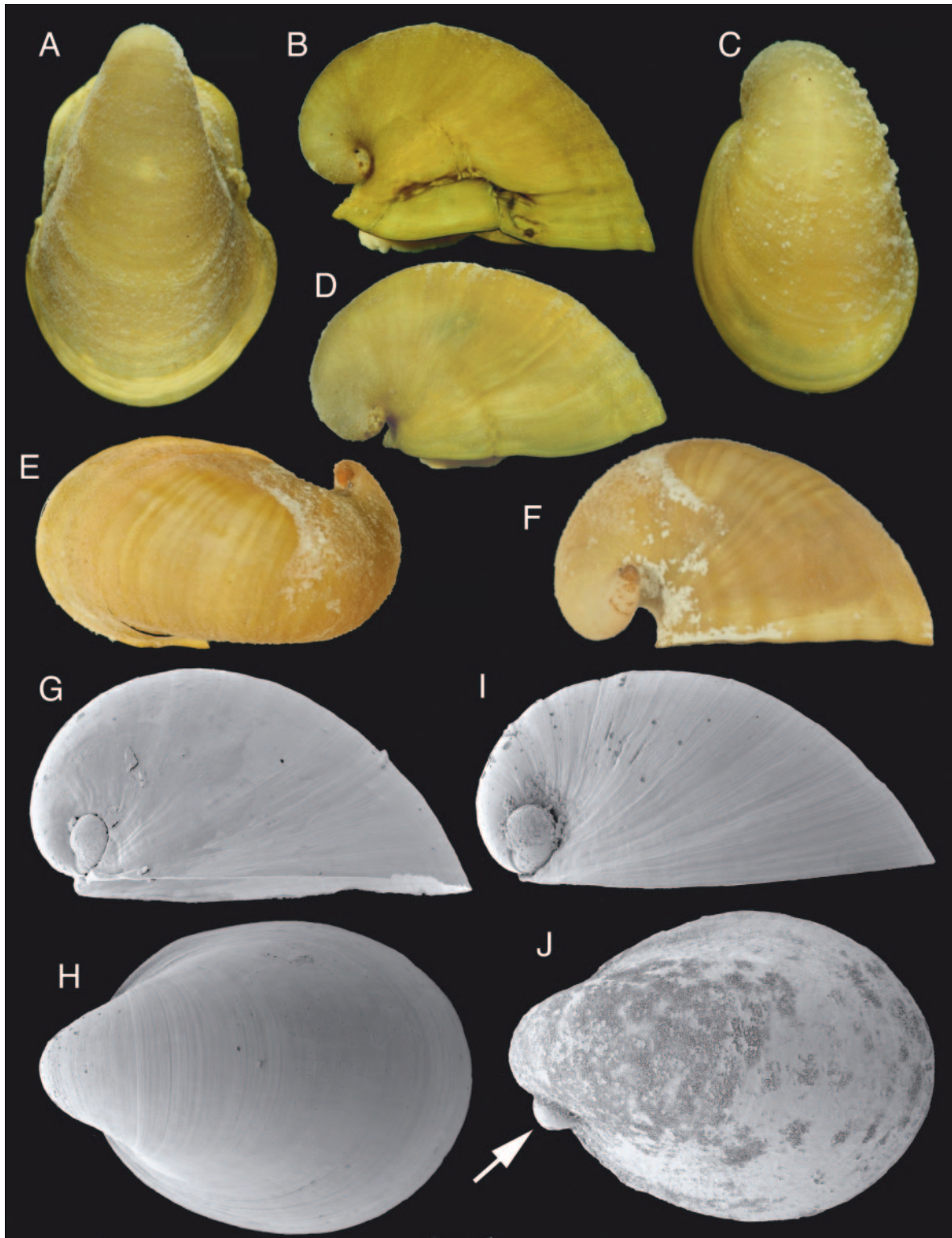


**Figure 3.** *Lepetodrilus* spp. (A–B) *L. gordensis*, holotype, shell length 11.8 mm. (C–D) *L. gordensis*, paratype, length 8.3 mm. (E–F) *L. fucensis*, Endeavour Segment, length 10.0 mm (SMNH 79537). (G–H) *L. fucensis*, young, Endeavour Segment, length 1.36 and 1.62 mm (SMNH 45610). (I–J) *L. gordensis*, young, shell length 1.07 and 1.14 mm, notice protruding larval shell at arrow (SMNH 52638).

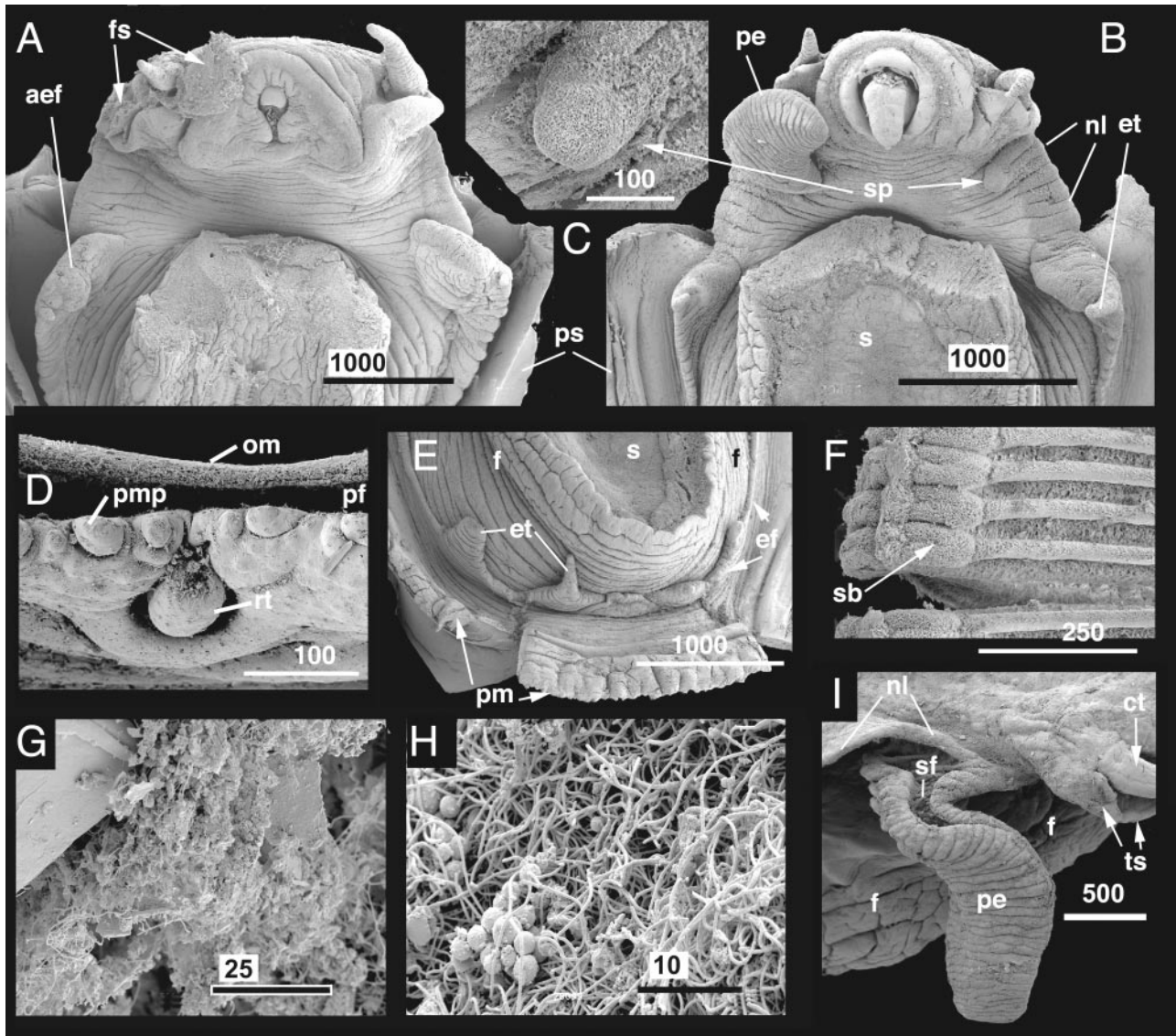


**Figure 4.** *Lepetodrilus* spp. (A) *L. gordensis*, female, head-foot; propodium removed to show neck. Notice absence of papilla. (B–C) *L. fucensis*, male, propodium removed. Notice sensory papilla, enlarged in (C). (D–I) *L. gordensis*. (D) Bilobed pallial margin with retractile tentacle. (E) Posterior part of foot with epipodial fold and tentacles. (F) Distal part of ctenidial filaments with sensory bursicles. (G) Pseudofeces (rejects from gill). (H) Detail of food string, mainly filamentous bacteria. (I) Right side of head-foot with neck lobe, penis, and cephalic tentacle. aef—anterior part of epipodial fold; ct—cephalic tentacle; ef—epipodial fold; et—epipodial tentacle; f—foot; fs—food string; nl—neck lobe; om—outer fold of pallial margin; pe—penis; pf—pallial furrow (where periostracum is formed); pm—pallial margin; pmp—pallial margin papilla; ps—pallial skirt; rt—retractile pallial tentacle; s—sole of foot; sb—sensory bursicle (position of opening); sf—seminal furrow; sp—sensory papilla; ts—tentacle sheath. Scale bars in  $\mu\text{m}$ .

Sciences (CAS 173171); and National Museum of Natural History, Washington (USNM 1083160).

Other material examined: SMNH #46609, 62679, 78769, *Tiburon* dive T186, 42° 45'N, 126° 42'W, 2716 m depth, 3 + 4 + 200 specimens; #62680, *Tiburon* dive T188, 42° 45'N, 126° 42'W, 2715 m depth, 7 specimens; #52638, *Tiburon* dive T454, 42° 45'N, 127° 42'W, 2696 m depth, 50 specimens.

*Lepetodrilus fucensis*: all from the Juan de Fuca Ridge:

SMNH #45611, *Jason* dive #258, Endeavour Segment, Quebec vent field, 47° 56'N, 129° 06'W, 1919 m depth, 5 specimens; SMNH #45610, *Jason* dive #286, Endeavour Segment, Easter Island, 47° 56'N, 129° 05'W, 2198, 10 specimens; #45840, *Jason* dive #310, Endeavour Segment, Raven field, 47° 58'N, 129° 05'W, 2163 m depth, 10 specimens; SMNH #45841, *Jason* dive #MAVS 60, Endeavour Segment, Raven Field, 47° 57'N, 129° 05'W,

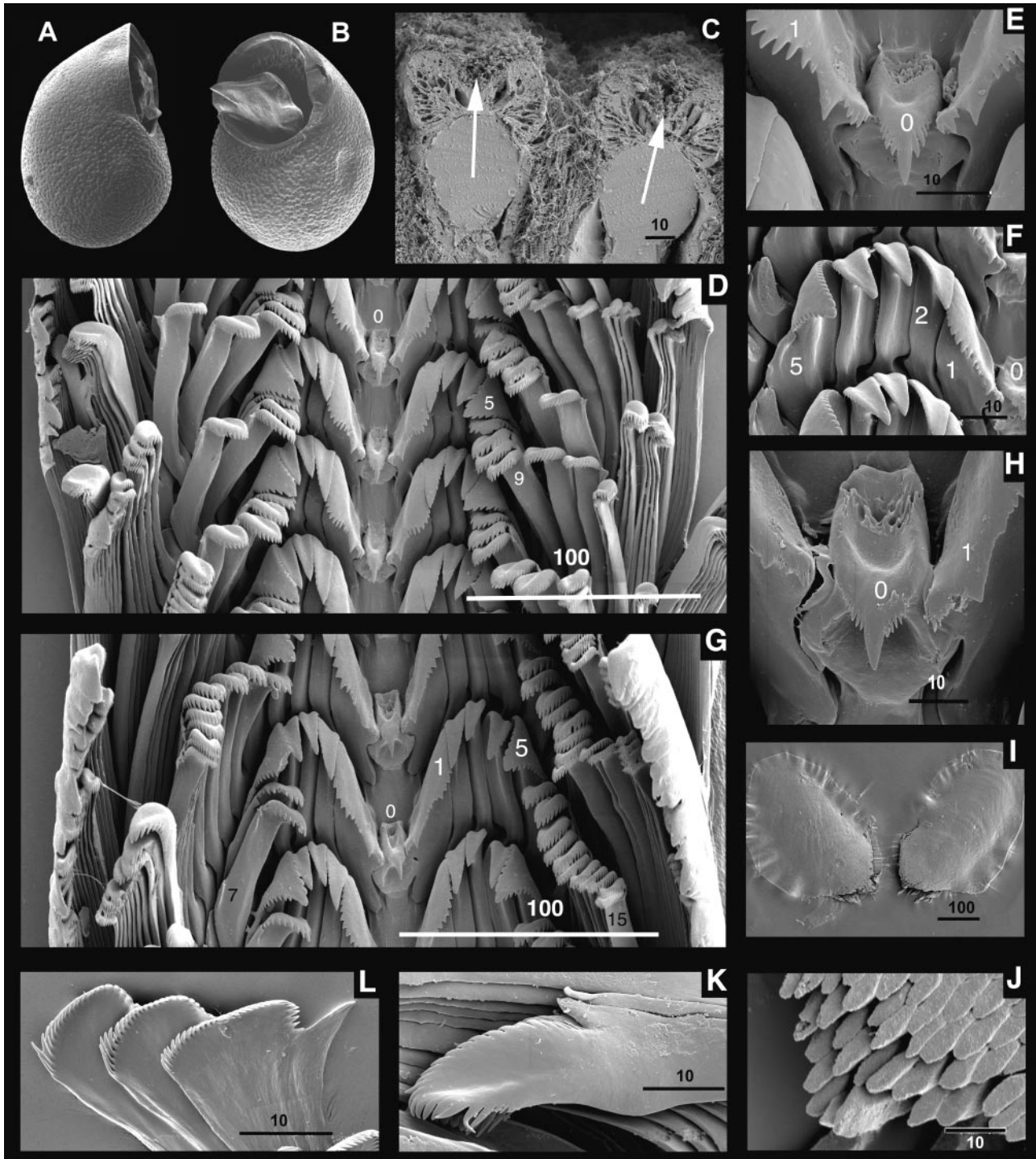


**Figure 5.** *Lepetodrilus* spp. (A–B) *L. fucensis*, recently settled larva, apical and ventral view, maximum shell diameter 175 μm. (C) *L. gordensis*, cross section of dorsal part of two ctenidial leaflets. Notice bilobed dorsal surface, furrow marked by arrow. (D–F) *L. fucensis*. (D) Whole width of radula. (E) Central tooth. (F) Lateral teeth. (G–I) *L. gordensis*. (G) Whole width of radula. (H) Central tooth. (I–J) Jaw and detail of its anterior margin. (K) Apical part of marginal teeth. (L) Outermost, broader marginal teeth. Numbers indicate sequential order of teeth with central tooth as 0. Scale bars in μm.

2180 m depth, 15 specimens; SMNH #79537, *Ropos* dive R590, Endeavour Segment Clam bed, 47° 57'N, 129° 05'W, 2200 m depth, 25 specimens; SMNH #79536, R591, Endeavour Segment, Clam bed, 47° 57'N, 129° 05'W, 2189 m depth, 20 specimens; SMNH #62677, *Tiburon* dive T180, Cleft, 44° 39'N, 130° 21'W, 2211 m depth, 6 specimens; SMNH #62678, *Tiburon* dive T184, Cleft, 44° 59'N, 130° 12'W, 2238 m depth, 6 specimens; SMNH #62681, *Tiburon* dive T458, Cleft, 44° 39'N, 130° 21'W, 2202 m depth, 7 specimens.

*Description of shell of L. gordensis n. sp. (Figs 3A–D, I–J)*

Shell forming an irregularly twisted cap-shaped bowl or cone with overhanging apex. Larval shell (Fig. 3I–J), maximum diameter 170–180  $\mu$ m, indistinctly coiled, with a finely and softly pitted surface; corroded already at shell diameter of 1 mm. Small specimens, up to shell diameter 2–3 mm, slightly asymmetrical, bowl-shaped, with 1/6 of apical coil displaced behind shell margin. Spire slightly displaced to left; protoconch protruding up to 2.5 mm shell length. Growing larger, shell becomes proportionally taller; at 5–6 mm, base starts to take shape after substrate. Adult specimens, shell length 8–13 mm, of highly variable shape with quite fragile shell, 1.4–1.8 times as long as high. Surface smooth except indistinct growth lines. Calcareous layer: thin, whitish; periostracum thick, greenish or brownish, inhabited by pustules or crusts of bacterial colonies.

*Dimensions*

Maximum shell length 13 mm; usually 8–11 mm.

*Soft parts*

Visceral hump very small and contains mainly pericardium and rearmost part of gonad. Gonad visible by transparency from outside (shell removed), in a posterior to ventral view, as small light structure, finely lobed, tubular and iridescent in male, coarsely granular and dull in female. Main volume of gonad situated more anteriorly, ventral to digestive gland.

Shell muscles well developed, surrounding early spire whorl, meeting posteriorly across columella and enclosing a large empty volume (actually the space between foot and spire in a coiled gastropod).

Pallial cavity large and spacious, pallial margin bilobed (Fig. 4D), inner lobe crenulated by single series of papillae and single retractile pallial tentacle just inside papillae, in front of left cephalic tentacle. Ctenidium attached dorsally along 3/4 and ventrally along 2/3 of its length; bipectinate; dorsal filaments short and triangular; left branchial chamber so small so there can hardly be water-flow of importance. Tips of leaflets swollen; contain a sensory bursicle (Fig. 4F).

Dorsal edge of filaments bilobed, with indistinct furrow from base to tip (Fig. 5C).

Foot large, ovate, anteriorly blunt, posteriorly rounded (Fig. 4E); propodium distinctly demarcated; except for the anterior portion surrounded by thin epipodial fold (Fig. 4E). Anterior end of epipodial fold ending in triangular, flat and fleshy epipodial flap with small finger-like tentacle (Fig. 4A); posteriorly a pair of flat lobes with small tentacles at each side of foot (Fig. 4E) and unpaired mid-lobe with no tentacle. Epipodial tentacles with apical tuft of cilia.

Head distinctly set off from head-foot, elongate, dorso-ventrally flattened (difference from most species of *Lepetodrilus*, which have short, more cylindrical, neck). Cephalic tentacles surrounded by and basally inserted in fleshy tentacle sheath (Fig. 4A, I); left one continues towards and encircles mouth, defining oral disc. Depending on state of preservation, oral disc may be well defined and surrounded by a rim, or poorly defined if the snout is less contracted. Cephalic tentacles of small (<1.5 mm shell length) specimens richly equipped with sensory papillae, barely noticeable in adult specimens.

Neck-lobe (Fig. 4A, I), a lateral, thick skin fold, starts at anterior end of epipodial fold and differs in structure from this by being thick, fleshy, and when contracted, transversely ridged. Right neck-lobe wider and drawn out to a point, in female a simple continuation that does not reach front of head; in male its anterior extension forms long, large, blunt tentacle with lateral, deep and ciliated gutter, starting at ventral side of lobe (Fig. 4I). No sensory neck papilla.

Esophagus wide and spacious. Stomach cylindrical, poorly set off, diameter barely twice diameter of intestine; situated basally in the small visceral hump; diameter 0.4 mm, length 1.0 mm in 10-mm specimen; anterior loop of intestine often visible by transparency after removal of pallial skirt and gill, trough back of head-foot; diameter of lumen 0.2 mm.

Radula (Fig. 5G–L). Most anterior teeth, especially rhachidian and innermost laterals always with slight signs of wear; total length 3 mm in a 7-mm male, width 0.4 mm. Formula: *ca* 30 - 5 - 1 - 5 - *ca* 30. Rhachidian (Fig. 5H) low and sturdily built, with prominent main and 3–6 smaller lateral cusps; posterior surface concave, partly hollow. Laterals (see Fig. 5F of *fucensis* which seems not to differ) tightly interlocking; first lateral 3 times as wide as subsequent ones; main cusp small but prominent; inner serration short and inconspicuous; outer serration distinctly curved, with *ca* 8 cusps. Second–fourth laterals: of similar size and shape, sturdily built, strongly curved with narrow, indistinctly serrate apical plate. Fifth lateral: much broader, with broadly triangular, bipartite apical plate. Inner marginals: sturdily built with rounded, serrate apical plate. Outer marginals: gradually more slender, with more narrow apical

plate. Serration of outer side finished by a distinct "spur." Outermost marginal is broad and membranaceous.

Jaws (Fig. 5I–J) paired, oval, maximum diameter 450  $\mu\text{m}$ , consisting of numerous prismatic elements.

### Biology

*Lepetodrilus gordensis* usually occurs in large numbers and often in stacks of up to half a dozen individuals, and the shell base of specimens larger than 4–6 mm usually is irregular, indicating a sedentary life. Some specimens have the gut filled by mineral particles, presumably reflecting grazing. Frequently, however, the esophagus and stomach is filled by masses of filamentous bacteria. These seem to be cultivated in the gill, between the leaflets, transported to the tips of the filaments, and over to the pallial skirt where mineral particles and mucus are separated (Fig. 4G) and discarded (pseudo feces) and the mass of bacteria (Fig. 4H) continues to the mouth *via* the right neck lobe. The good condition and slight degree of wear of the anterior part of the radula, both in *L. fucensis* and *gordensis*, indicate that it is not used for scraping the substrate to the same extent as in other species of *Lepetodrilus*, something that hardly is possible when living in stacks. Therefore, filter-feeding, symbiotic bacteria, or both probably largely supply their nourishment.

### Etymology

Name derived from the Gorda Ridge.

### Discussion

The genus *Lepetodrilus* belongs to the Lepetodrilidae, superfamily Lepetodrilioidea, with some 13 species living in hydrothermal vents (Warén and Bouchet, 2001). Recently a few additional species have been found in methane and sulfide seeps (Warén, unpubl.), and a piece of wood from 21°N was found to be the home of many specimens of *L. cf. elevatus* McLean, 1988 (Johnson, unpubl.) As far as known, *L. gordensis* - *fucensis* is the only exception to an exclusively grazing feeding style.

*L. fucensis* was first mentioned by de Burgh and Singla (1984; as "new limpet species"), who reported symbiotic bacteria from its gill. McLean (1988) named and described the species from the Juan de Fuca Ridge; Fretter (1988) described its anatomy; and McLean (1993) reported it from the Gorda Ridge. These descriptions are quite exhaustive but the species is now better known, more material is available from a wider range of localities, and a better comparative background exists. Therefore we supplement earlier reports, with comments and information from our material.

*Lepetodrilus fucensis* (incl. *gordensis*) has been mentioned in several ecology papers from these two areas since

it is usually the numerically dominant macrofauna in vent localities on the Juan de Fuca and Gorda ridges; densities of 100,000 specimens per square meter have been reported (Tsurumi and Tunnicliffe, 2001). These high densities are explained not only by the presence of many young specimens, but also by the fact that members of the species live in stacks, a mode of life typical for several filter-feeding gastropods of the family Calyptraeidae (Collin, 1995). This provides better access to unfiltered water and presumably also to sulfides for the symbiotic bacteria.

Our examination revealed at least four differences in morphology:

(1) Absence of a sensory papilla of the ventral side of the head of *L. gordensis* (Fig. 4A). This papilla was described and assigned a sensory function by Fretter (1988) in *L. fucensis* (Fig. 4B–C). It is a distinctly set off, tall papilla close to the basis of the left tentacle sheath, with a ciliated patch on its tip. We have confirmed its presence in more than a hundred specimens of *L. fucensis*, as well as its absence in *L. gordensis*. This observation was also verified by V. Tunnicliffe and A. Bates (University of Victoria, BC, Canada; pers. comm.).

(2) The dorsal edge of the ctenidial filaments is equipped with a furrow in *L. gordensis* (Fig. 5C). This is most easily visible in cross sections or in alcohol specimens; when critical-point-dried, the furrow is partly concealed by the cilia. A. Bates pointed this out to us.

(3) The shape of the adult shell is more irregular and the spire more openly coiled in *L. fucensis* than in *L. gordensis* (Fig. 1A–F).

(4) Small specimens, 0.7–2.5 mm shell length, can be distinguished by *L. gordensis* having a spire that is slightly twisted over to the left side, and having the larval shell visible as a small bulge at the right side of the spire when placed on a horizontal surface (Fig. 3I–J). In *L. fucensis* the protoconch does not protrude, and the shell is almost perfectly symmetrical at this size (Fig. 3G–J).

Our specimens of *L. fucensis* from the Cleft Area (JdF) have a brownish periostracum and deep purplish color of the inside of the shell. In most other localities (Juan de Fuca and Gorda ridges) the periostracum is greenish and the shell white. This is a variation we have noticed in several species of *Lepetodrilus*, but its significance or origin remains unknown.

Fretter (1988) considered the neck lobes to be prolongations of the "epipodial folds." This is not correct. Examination of a growth series (from 0.3 mm) shows that the right lobe is derived from the neck tentacle of newly settled specimens, while the epipodial fold and its fleshy tentacles develop later (0.8–1.2 mm), starting as a ridge on the side of the foot. A left neck tentacle is often developed in vetigastropods and is known to be the starting point of the left neck lobe when present, and we assume a parallel origin in *Lepetodrilus* (Warén, unpubl.).

De Burgh and Singla (1984) pointed out symbiosis with bacteria when they observed superficial endocytosis on the gill of *L. fucensis*. However, the massive amounts of bacteria between the gill filaments and the grazing of some specimens (mainly small) shows a high variation in feeding biology of the two species, probably in response to environmental conditions. We cannot say which factors direct the type of feeding, except that life in a stack probably prohibits grazing and promotes suspension feeding.

The larval shell of *L. fucensis* has not been illustrated, so we include Figure 5A–B. McLean (1988) reported a larval shell diameter of 120  $\mu\text{m}$ , probably a slip of the pen since our measurements of both species gave 170–180  $\mu\text{m}$  in largest diameter. Furthermore, Fretter (1988) reported an egg diameter (in the oviduct) of 100–140  $\mu\text{m}$ , which fits our results. The

larval shells of *L. fucensis* and *gordensis* are very similar to each other; all other species of *Lepetodrilus* have a more coarsely sculptured larval shell. It can be safely assumed that the species has a free-swimming dispersal phase since larvae of *L. fucensis* have been captured in the plumes of the vents (Mullineaux *et al.*, 1995); other *Lepetodrilus* species were reported by Kim and Mullineaux (1998) from plankton as well as in sediments traps. Nothing is known about the length of the planktonic life—neither the minimum time for development of a competent larva (important for local recruitment), nor the maximum lifespan (important for dispersal between hydrothermal areas). Possibly the larvae are able to delay settlement for a long time to survive by drifting with bottom currents in a hibernating condition, as shown for polychaete worms (Pradillon *et al.*, 2001).